

Supplementary Data

Bioinspired therapeutic platform based on extracellular vesicles for prevention of arterial wall remodeling in hypertension

Chen Wang^{a, 1}, Changyang Xing^{a, 1}, Zhelong Li^a, Yunnan Liu^a, Qiaoying Li^a, Yixiao Wang^a, Jiao Hu^a, and Lijun Yuan^{a,**}, Guodong Yang^{b,c,*}

^aDepartment of Ultrasound Diagnostics, Tangdu Hospital, Fourth Military Medical University, Xi'an, 710038, People's Republic of China.

^bState Key Laboratory of Cancer Biology, Fourth Military Medical University, Xi'an, 710032, People's Republic of China.

^cDepartment of Biochemistry and Molecular Biology, Fourth Military Medical University, Xi'an, 710032, People's Republic of China.

¹These authors contributed equally to this study.

*Correspondence authors:

*Guodong Yang, Department of Biochemistry and Molecular Biology, Fourth Military Medical University, Changlexi Road NO.169th, 710032, Xi'an, People's Republic of China. Email: yanggd@fmmu.edu.cn

**Lijun Yuan, Department of Ultrasound Diagnostics, Tangdu Hospital, Fourth Military Medical University, Xinsi Road NO.569th, 710038, Xi'an, People's Republic of China. Email: yuanlj@fmmu.edu.cn

Table S1. Primers/miRNA/mRNA sequences used in this study

Mimics/Inhibitors	Sequence (5'-3')	
<i>cel</i> -miR-54-5p mimics	Sense AGGAUAUGAGACGACGAGAACA Antisense UUCUCGUCGUCUCAUAUCCUUU	
miR-320d mimics	Sense AAAAGCUGGGUUGAGAGGA Antisense CUCUCAACCCAGCUUUUUU	
miR-423-5p mimics	Sense UGAGGGGCAGAGAGCGAGACUUU Antisense AGUCUCGCUCUCUGCCCCUCAU	
N.C. mimics	Sense UUCUCCGAACGUGUCACGUTT Antisense ACGUGACACGUUCGGAGAATT	
miR-320-inhibitor	CCCUCUCAACCCAGCUUUU	
miR-423-5p-inhibitor	AAAGUCUCGCUCUCUGCCCCUCA	
N.C. inhibitor	CAGUACUUUUGUGUAGUACAA	
PCR primers	Forward (5'-3')	Reverse (5'-3')
miR-320d	AAAAGCTGGGTTGAGAGG	Provided in the kit
miR-320-inhibitor	CCCTCTCAACCCAGCTTT	
miR-423-5p	TGAGGGGCAGAGAGCGAGACTTT	
miR-423-5p-inhibitor	AAAGTCTCGCTCTCTGCCCTCA	
U6	CTCGCTTCGGCAGCAC A	
<i>cel</i> -miR-54-5p	AGGATATGAGACGACGAGAACA	
<i>m-Spp1</i>	AGCAAGAACTCTTCC AAGCAA	GTGAGATTCGTCAGATTCATCCG
<i>m-Col3a1</i>	CTGTAACATGGAACTGGGAAA	CCATAGCTGAACTGAA AACCACC
<i>m-Coll1a1</i>	GCTCCTCTTAGGGGCCA CT	CCACGTCTCACCATTGGGG

<i>m-Mybl2</i>	TCTGGATGAGTTACACT ACCAGG	GTGCGGTTAGGAAAGT GACTG
<i>m-Gapdh</i>	AGGTCGGTGTGAACGG ATTTG	TGTAGACCATGTAGTTG AGGTCA
<i>r-Spp1</i>	GATGACGACGACGATG ACGA	GCTGGCAGTGAAGGAC TCAT
<i>r-Col3a1</i>	AGCTGGTCAGCCTGGA GATA	GAGGGCCATGTTCCACC TCTC
<i>r-Coll1a1</i>	GAGAGGTGAACAAGGT CCCG	CAAGGTCTCCAGGAAC ACCC
<i>r-Gapdh</i>	TTCACCACCATGGAGA AGGC	CTCGTGGTTCACACCC ATCA

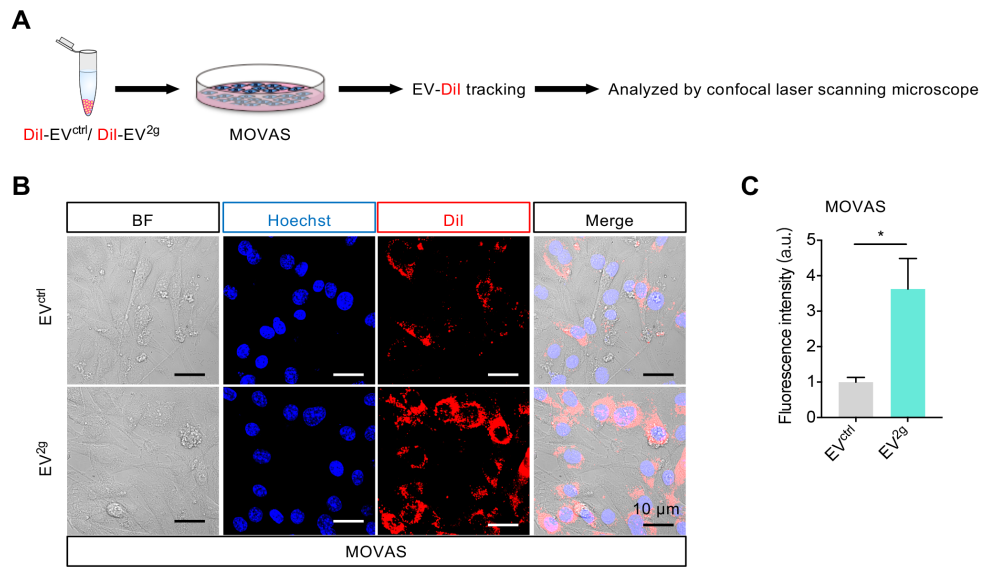


Figure S1. Uptake of EC derived EVs by SMCs.

(A) Schematic illustration of the experimental procedure. (B) Confocal images of the DiI-labeled EV (red) localization in the MOVAS. Nuclei were counterstained with Hoechst. Scale bar = 10 μm. (C) Quantification of the DiI fluorescence intensity in different groups of MOVAS. Data were shown are representative of 3 independent experiments and presented as mean ± SEM. * $P < 0.05$ as determined by t test.

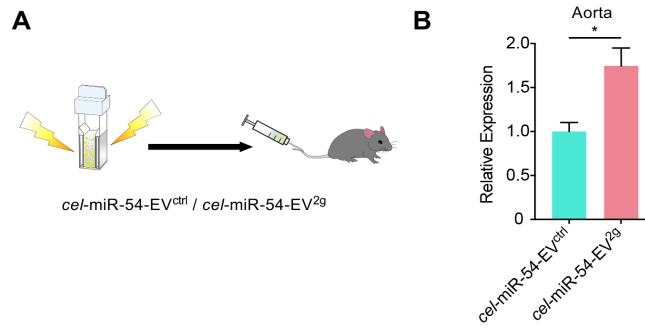


Figure S2. Distribution of EV^{ctrl} and EV^{2g} in the artery.

(A) Schematic illustration of the experimental procedure. *cel*-miR-54 loaded EVs were injected via tail vein. (B) Expression of *cel*-miR-54 in aorta after injection of *cel*-miR-54 loaded EVs. Data were expressed as mean \pm SEM. n = 3. * $P < 0.05$ as determined by *t* test.

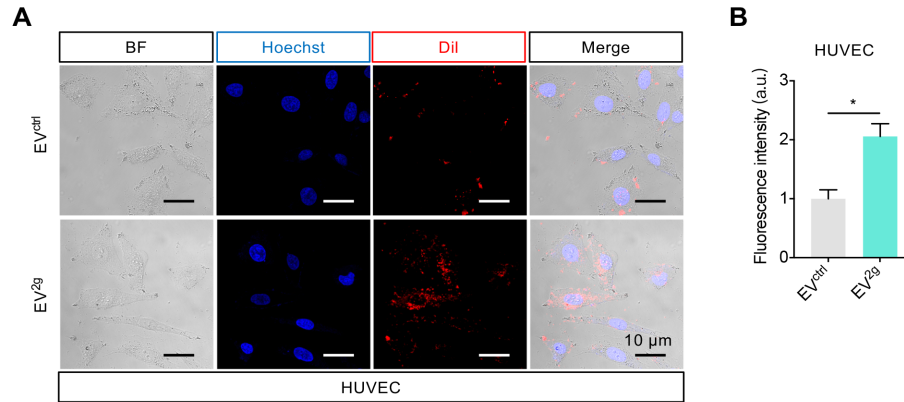


Figure S3. Uptake of EC derived EVs by endothelial cells.

(A) Confocal images of the DiI-labeled EV (red) localization in the HUVEC. Nuclei were counterstained with Hoechst. Scale bar = 10 μ m. (B) Quantification of the DiI fluorescence intensity in different groups of HUVEC. Data were shown are representative of 3 independent experiments and presented as mean \pm SEM. * P < 0.05 as determined by t test.

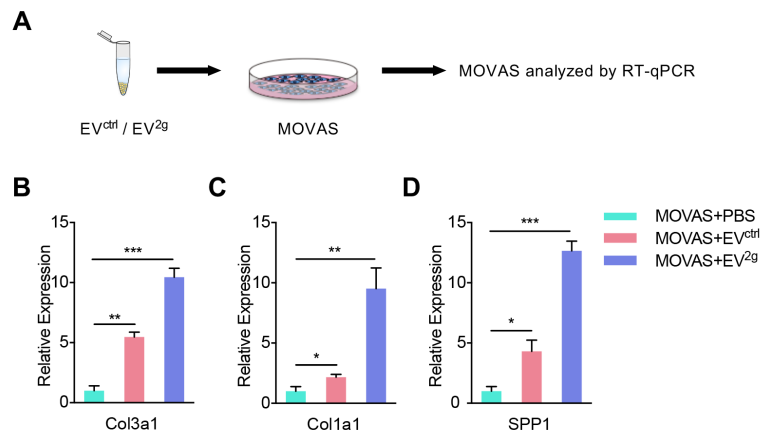


Figure S4. The effects of EV^{ctrl} and EV^{2g} on the smooth muscle cells.

(A) Schematic illustration of the experimental procedure. (B-D) Expression of *Col3a1* (B), *Colla1* (C) and *Spp1* (D) in MOVAS treated with PBS, EV^{ctrl} and EV^{2g}. Expression of mRNA candidates were normalized to *Gapdh* expression. Data are expressed as mean ± SEM of at least 3 independent experiments. n.s., no significance, * $P < 0.05$, ** $P < 0.01$, *** $P < 0.001$ by one-way ANOVA.

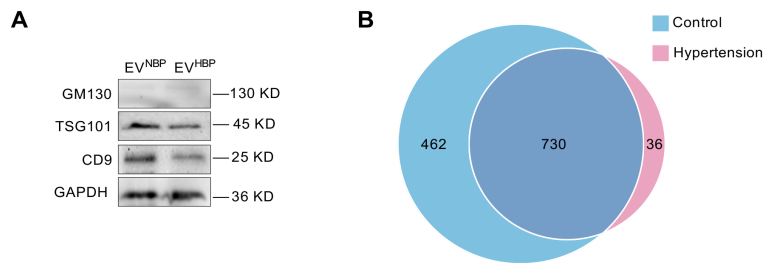


Figure S5. Characterization of the isolated EVs from NBP and HBP subjects, and profiling of the differential EV-miRNAs.

(A) Western blot analysis of EV inclusive and exclusive markers in plasma of blood samples from NBP and HBP, including GM130, TSG101 and CD9. Representative data of at least 3 independent experiments. (B) Venn chart of differentially expressed EV-miRNAs screened out between NBP versus HBP. NBP, normal blood pressure; HBP, high blood pressure (hypertension).

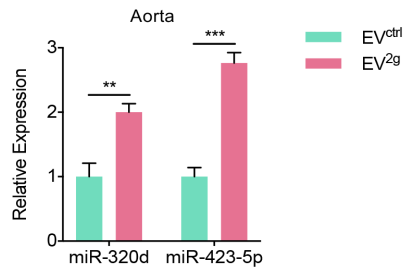


Figure S6. EVs derived from dysfunctional EC transfer the miRNA candidates to the aorta.

Expression of miR-320d and miR-423-5p in vascular after the injection of EV^{ctrl} and EV^{2g}. Expression of miRNA candidates were normalized to *U6* expression. Data are expressed as mean \pm SEM. $n = 3$. ** $P < 0.01$, *** $P < 0.001$ by *t* test.

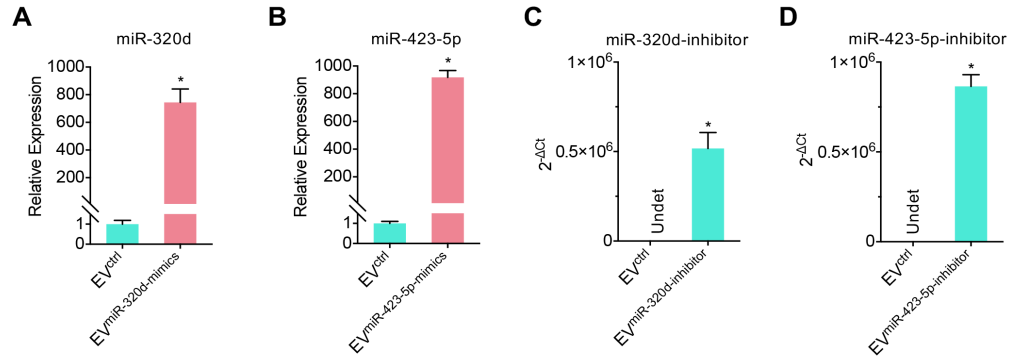


Figure S7. The miRNA loading efficiency into the EVs.

(A-B) Expression of miR-320d-mimics and miR-423-5p-mimics in EVs after the electroporation of the mimics respectively. Expression of miRNA candidates were normalized to *U6* expression. Relative expression was calculated using $2^{-\Delta\Delta C_t}$ method. (C-D) Expression of miR-320d-inhibitor and miR-423-5p-inhibitor in EVs after the electroporation of the inhibitors respectively. Relative expression was calculated by using $2^{-\Delta C_t}$ method. Data are expressed as mean \pm SEM. n = 3. * $P < 0.05$ by *t* test.

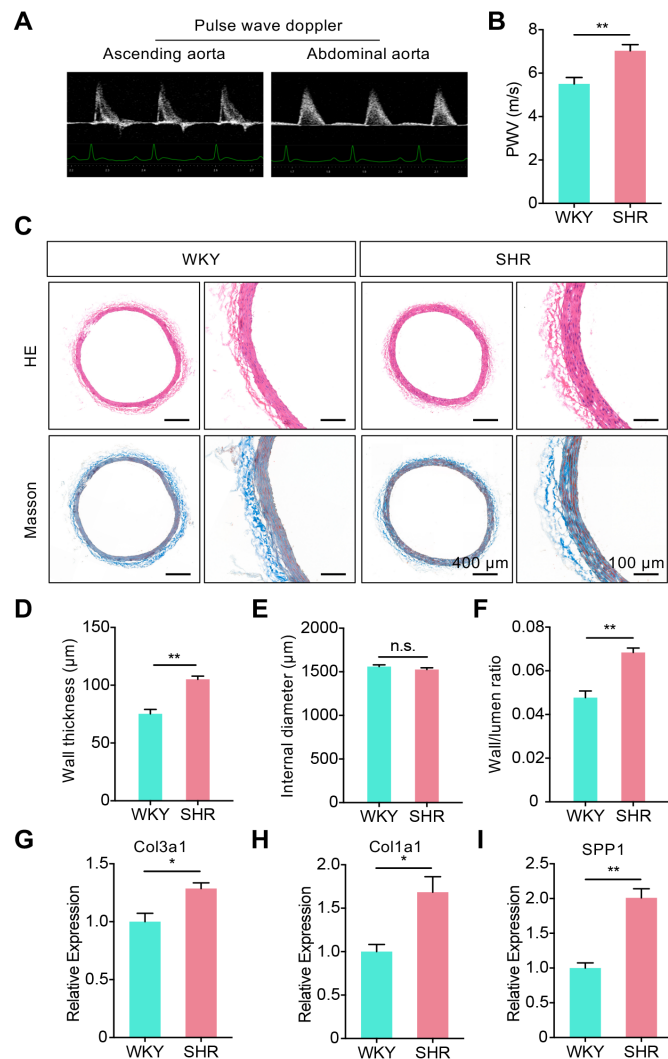


Figure S8. Arterial remodeling in SHR rats.

(A) Representative images showing the doppler spectra acquired at the ascending aorta and abdominal aorta, with the simultaneous ECG. (B) The PWV of control WKY rats and SHR rats. Data are means \pm SEM. $n = 5$. $**P < 0.01$ by t test. (C) Vascular changes as revealed by Hematoxylin/ eosin staining and Masson's trichrome staining of the aorta in WKY and SHR. Representative images of at least 3 rats of each group. Scale bars represent 400 μm or 100 μm respectively. (D-F) Wall thickness (D), internal diameter (E) and wall/ lumen ratio (F) of the aorta in WKY or SHR rats. n.s., no significance, $**P < 0.01$ as determined by t test. (G-I) Expression of *Col3a1*(G), *Col1a1* (H) and *Spp1* (I) in the aorta of WKY or SHR rats. Expression of mRNA candidates was normalized to *Gapdh* expression. Data are

expressed as mean \pm SEM. n = 3. * P < 0.05, ** P < 0.01 by t test.

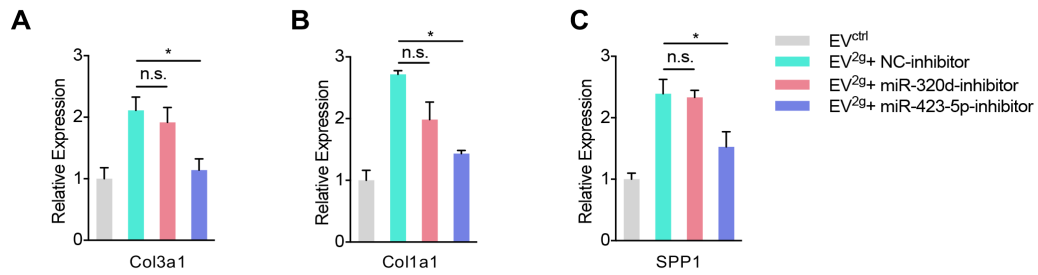


Figure S9. Effects of miR-320d and miR-423-5p on the synthetic phenotype of SMCs.

(A-C) Expression of *Col3a1* (A), *Col1a1* (B) and *Spp1* (C) in the MOVAS treated by EV^{ctrl}, EV^{2g} and EV^{2g} additionally treated with miR-320d-inhibitor and miR-423-5p-inhibitor transfection. Expression of mRNA candidates was normalized to *Gapdh* expression. Data are expressed as mean \pm SEM of at least 3 biological replicates. n.s., no significance, * $P < 0.05$ by one-way ANOVA.

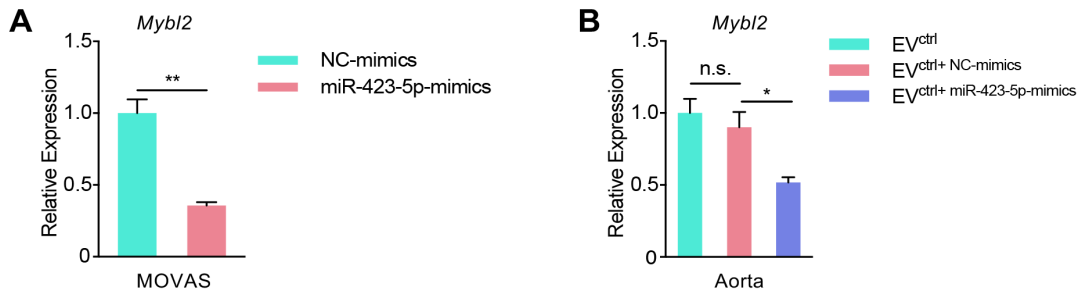


Figure S10. Inhibition of *Mybl2* by miR-423-5p.

(A) qPCR analysis of the expressions of *Mybl2* mRNA in MOVAS transfected with NC-mimics or miR-423-5p-mimics. Data are expressed as mean \pm SEM. $n = 3$. $**P < 0.01$ by t test. (B) qPCR analysis of the expressions of *Mybl2* mRNA in aorta from the mice treated with indicated EVs. Expression of mRNA candidates was normalized to *Gapdh* expression. Data are expressed as mean \pm SEM. $n = 3$. n.s., no significance, $*P < 0.05$ by one-way ANOVA.